Heliyon 10 (2024) e35972

Contents lists available at ScienceDirect

Heliyon

journal homepage: www.cell.com/heliyon

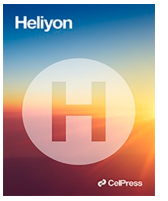

Research article

Constructing condylar cartilage organoid to explore primary cilia functions

Zhan Liu [a,1], Haoyu Zhou [a,1], Qingwei Wu [a], Tianhao Luo [a], Hanlin Tu [a], Guoliang Sa [a,b,**], Xuewen Yang [a,b,*]

[a] State Key Laboratory of Oral & Maxillofacial Reconstruction and Regeneration, Key Laboratory of Oral Biomedicine Ministry of Education, Hubei Key Laboratory of Stomatology, School & Hospital of Stomatology, Wuhan University, PR China
[b] Department of Oral and Maxillofacial Surgery, Hospital of Stomatology, Wuhan University, Wuhan, PR China

ARTICLE INFO

Keywords:
Condylar cartilage organoid
Primary cilia
IFT88
RNA sequencing
Hedgehog signaling pathway

ABSTRACT

An organoid culture system better recapitulates the cellular structure, function, and interaction between cells and the extracellular matrix (ECM) than a two-dimensional (2D) culture system. We here constructed a condylar cartilage organoid to explore the regulatory role of primary cilia. Similar to the natural condylar cartilage, the condylar cartilage organoid exhibited abundant ECM and comprised superficial, proliferative, and hypertrophic zones. Primary cilia in the condylar cartilage organoid were shorter on average than those in the 2D culture chondrocytes, but their average length was equivalent to those in the natural condylar cartilage. Notably, primary cilia in each zone of the condylar cartilage organoid had an average length similar to that of primary cilia in the natural condylar cartilage. According to transcriptomic and biochemical analyses, the expression of cilia-related genes and cilia-related Hedgehog (HH) signaling differed between the condylar cartilage organoid and 2D culture systems. *IFT88* knockdown promoted the protein levels of COL-X, TRPV4, and HH signaling molecules in the condylar cartilage organoid, but decreased them in the 2D culture system. Notably, the protein levels of COL-X, TRPV4, and HH signaling molecules increased in the superficial zone of the si *IFT88* condylar cartilage organoid compared with the condylar cartilage organoid. However, the protein levels of aforementioned molecules were not significantly different in proliferative and hypertrophic zones. Collectively, we successfully constructed the condylar cartilage organoid with a better tissue structure and abundant ECM. Moreover, the condylar cartilage organoid is more suitable for exploring primary cilia functions.

* Corresponding author. State Key Laboratory of Oral & Maxillofacial Reconstruction and Regeneration, Key Laboratory of Oral Biomedicine Ministry of Education, Hubei Key Laboratory of Stomatology, School & Hospital of Stomatology, Wuhan University, No. 237, Luoyu Road, Hongshan District, Wuhan, PR China.

** Corresponding author. State Key Laboratory of Oral & Maxillofacial Reconstruction and Regeneration, Key Laboratory of Oral Biomedicine Ministry of Education, Hubei Key Laboratory of Stomatology, School & Hospital of Stomatology, Wuhan University, PR China.

E-mail addresses: guoliang@whu.edu.cn (G. Sa), yxw._1962@whu.edu.cn (X. Yang).

[1] Authors contributing equally to this article.

https://doi.org/10.1016/j.heliyon.2024.e35972
Received 23 February 2024; Received in revised form 6 August 2024; Accepted 7 August 2024
Available online 13 August 2024

1. Introduction

Traditional two-dimensional (2D) monolayer cell cultures are widely used in biomedical research, such as for cell function and drug safety evaluation. However, the 2D culture system is unsuitable for studying tissue development and the interaction between cells and the extracellular matrix (ECM) [1,2]. In the 2D culture system, the lack of cell–ECM interaction alters several biological processes, including cell proliferation, migration, and apoptosis [3,4]. This may be among the major reasons for the conflicting results of *in vitro* and *in vivo* experiments. For example, knockout of Yes-associated protein and transcriptional coactivator with PDZ-binding motif genes impaired murine chondrocyte proliferation *in vitro*. However, cartilage-specific knockout of the aforementioned genes marginally affected chondrocyte proliferation *in vivo* [5].

Many studies have focused on constructing organoid culture systems to overcome the aforementioned limitations of 2D culture systems [6]. These organoid systems can model the tissue architecture and complexity and be extensively used in many translational applications such as regenerative medicine, development research, and precision medicine [1,7]. Organoid culture systems preserve the natural tissue structure and ECM components compared with 2D culture systems and are therefore more advantageous in mimicking the *in vivo* microenvironment and reproducing physiologically relevant cell−microenvironment interactions. Moreover, cellular functions, such as receiving extracellular microenvironment signals and mediating signal transduction, are also different in organoid and 2D culture systems because of ECM re-establishment [8,9].

Many organs such as the liver, gut, and brain have been cultured using the organoid system [7,10]. Applying the organoid system to skeletal systems has also been explored. For example, the self-assembling knee cartilage was successfully constructed using the organoid culture and used for drug discovery. It exhibited prospects for application in regenerative medicine [11,12]. According to these advantages, condylar cartilage organoids may be a more appropriate platform for studying condylar cartilage development and regeneration. However, the construction of condylar cartilage organoids and related research are lacking.

Based on the understanding gathered from the previously constructed knee cartilage, we here constructed a novel condylar cartilage organoid by using condylar chondrocytes from Sprague–Dawley (SD) rats [13,14]. The condylar cartilage organoid preserved the condylar cartilage's natural organization and hierarchical structure and exhibited abundant ECM. ECM deposition in chondrocytes is closely associated with primary cilia [15,16]. Therefore, the primary cilia length between the condylar cartilage organoid and the 2D culture system was evaluated through immunofluorescence. To determine whether cilia-related genes and signaling transduction were also changed in the condylar cartilage organoid compared with 2D culture systems, RNA sequencing (RNA-seq) was performed. The expression of primary cilia-related genes was compared between the condylar cartilage organoid and 2D culture systems. We also attempted to elucidate whether primary cilia between the condylar cartilage organoid and 2D culture exerted a different effect on ECM deposition through these cilia-related genes and pathways.

Altogether, the findings highlight that the condylar cartilage organoid can better present the natural condylar cartilage structure than the 2D culture. The regulatory roles of primary cilia in condylar chondrocytes differed drastically between the condylar cartilage organoid and 2D culture systems.

2. Results

1. Successful construction of the condylar cartilage organoid

Condylar chondrocytes from the SD rats were seeded into agarose wells. After 1 or 2 days, the chondrocytes aggregated and formed a cellular mass. The thickness of the mass gradually increased, whereas its diameter gradually decreased on days 0–7. The mass gradually grew into the condylar cartilage organoid on days 7–10. The diameter of the organoid was 2–3 mm (Fig. 1A).

Hematoxylin and eosin (HE), Safranin O, and Sirius Red staining presented the structure of the condylar cartilage organoid. HE staining revealed that the condylar cartilage organoid had a hierarchical structure and was segregated into three cellular zones (superficial, proliferative, and hypertrophic zones) from the outside to the inside. This structure was similar to that of the natural condylar cartilage (Fig. 1B). Safranin O staining unveiled that aggrecan was concentrated in the superficial and hypertrophic zones of the condylar cartilage organoid, similar to that observed within the natural condylar cartilage (Fig. 1C). After Sirius Red staining, collagen fiber positivity was observed in the superficial and hypertrophic zones of the condylar cartilage organoid (Fig. 1D), similar to that observed within the natural condylar cartilage. Immunohistochemical staining unveiled type II collagen (COL2A1) positivity in the three zones of the condylar cartilage organoid, similar to that observed within the natural condylar cartilage (Fig. 1E).

2. Abundance of ECM in the condylar cartilage organoid is associated with primary cilia

Primary cilia are crucial mediators of ECM deposition [17,18]. Considering that ECM was abundant in the condylar cartilage organoid compared with the 2D culture chondrocytes, we speculated that the morphology and function of primary cilia also changed. Therefore, primary cilia length was compared among the 2D culture chondrocytes, condylar cartilage organoid, and natural condylar cartilage through confocal microscopy. Primary cilia were marked with IFT88 and acetylated-α-tubulin (Ac-α-tubulin) [19]. On average, primary cilia were longer in the 2D culture system than in the condylar cartilage organoid and natural condylar cartilage (Fig. 2A–C, E, G). Meanwhile, the average primary cilia length in the condylar cartilage organoid and natural condylar cartilage was similar (Fig. 2C–E, G). Moreover, similar to that in the natural condylar cartilage, primary cilia length differed in each zone of the condylar cartilage organoid, with the longest and shortest cilia observed in the hypertrophic and superficial zones, respectively (Fig. 2C, D, E, F, H, I).

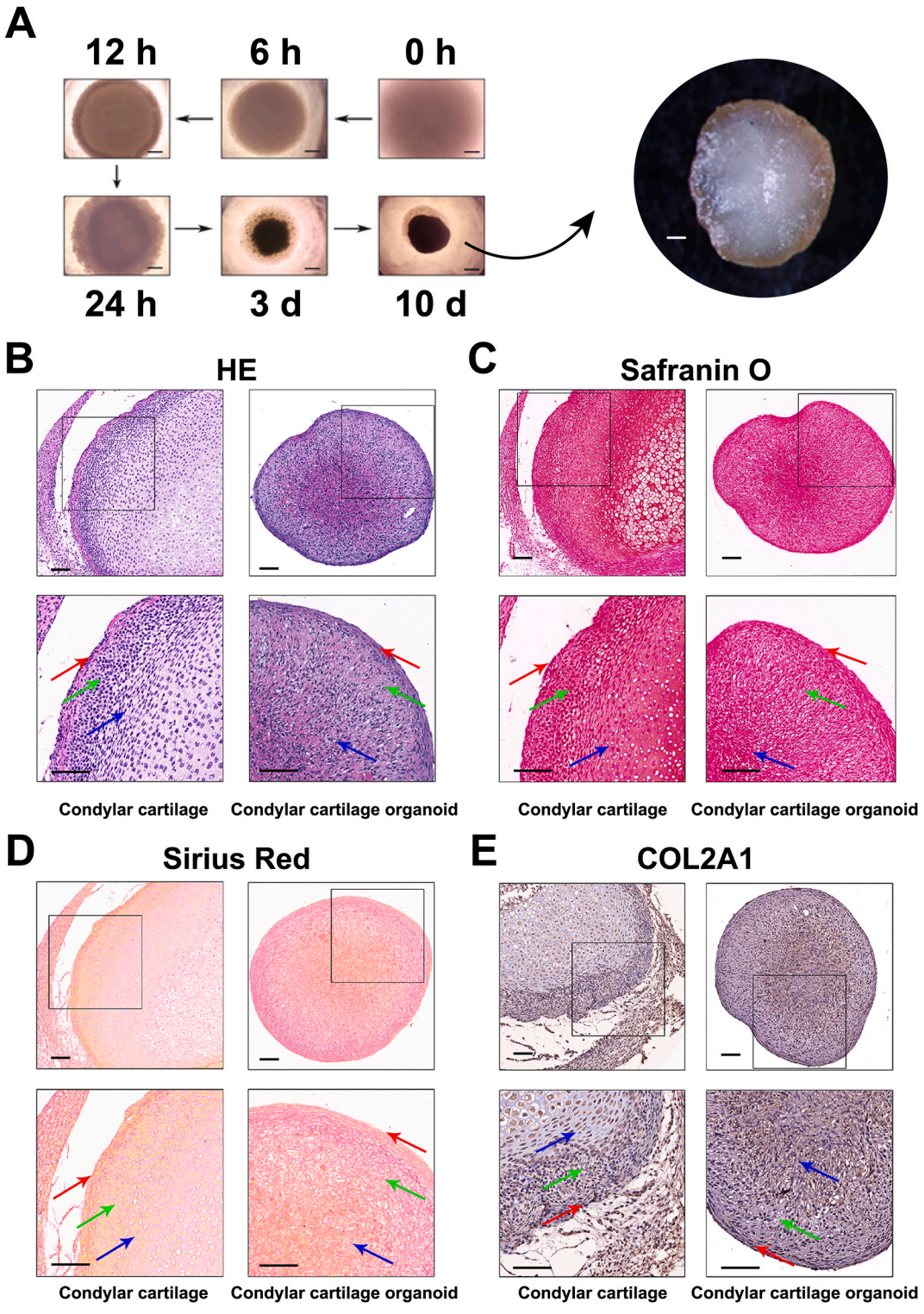

(caption on next page)

Fig. 1. The histological features of condylar cartilage organoid.
Panels A display the formation of condylar cartilage organoid after condylar chondrocytes were seeded. (B) HE staining of condylar cartilage organoid and natural condylar cartilage. Red, green, and blue arrows indicate the superficial zone, proliferative zone, and hypertrophic zone, respectively. (C) Safranin O staining indicates that aggrecan is concentrated in the superficial zone and hypertrophic zone of condylar cartilage organoid and natural condylar cartilage. (D) Sirius Red staining shows that collagen fibers concentrate in the superficial zone and hypertrophic zone of condylar cartilage organoid and natural condylar cartilage. (E) Immunohistochemical staining results show COL2A1-positive staining concentrates in the superficial, proliferative, and hypertrophic zones of condylar cartilage organoid and natural condylar cartilage. Scale bars = 100 μm.

3. RNA-seq reveals different expression of cilia-related genes and signaling pathways in the condylar cartilage organoid

Because primary cilia were shorter in the condylar cartilage organoid than in the 2D culture chondrocytes, we speculated that the expressions of cilia-related genes also changed. The expressions of primary cilia-related genes between the condylar cartilage organoid and 2D culture system were compared through RNA-seq. Moreover, RNA-seq identified 4253 differentially expressed genes between the condylar cartilage organoid and 2D culture (Fig. 3A). Overall, 71 and 69 cilia-related genes were upregulated and downregulated, respectively (Fig. 3B). We focused on IFT-related genes between the condylar cartilage organoid and 2D culture chondrocytes considering that they are fundamental carriers of the cilia function [20,21] (Fig. 3C). Regarding the IFT-related genes, a heatmap unveiled that the downregulated genes belonged to the IFT-B complex, while the most upregulated genes belonged to the IFT-A complex. Exceptionally, IFT88, a necessary component of the IFT-B complex, was also significantly upregulated. Furthermore, according to GSEA, the expressions of HH, canonical-Wnt, and Notch signaling pathways were upregulated in the condylar cartilage organoid compared with the 2D culture system (Fig. 3D). These signaling pathways were also associated with primary cilia [20,22,23]. This indicated that the primary cilia function altered between the condylar cartilage organoid and 2D culture system.

4. Primary cilia differentially regulate ECM deposition between the condylar cartilage organoid and 2D culture chondrocytes

Because the expressions of cilia-related genes and signaling pathways were altered in the condylar cartilage organoid, Gene Ontology (GO) analysis was performed to investigate whether cellular functions were altered. The GO analysis discovered the change in ECM structural constituents between the condylar cartilage organoid and 2D culture (Fig. 4A and B). This indicated that primary cilia differentially regulated ECM deposition between the condylar cartilage organoid and 2D culture. First, the IFT88 protein levels in the condylar cartilage organoid and 2D culture chondrocytes were detected. Confocal microscopy unveiled that the protein levels were upregulated in the condylar cartilage organoid compared with the 2D culture system (Fig. 5A). In western blotting, the IFT88 protein levels increased 30%–40 % in the condylar cartilage organoid compared with the 2D culture system (Fig. 5B and C). The impact of *IFT88* knockdown on ECM deposition was explored in the condylar cartilage organoid and 2D culture system. *IFT88* knockdown upregulated the COL-X protein level in the condylar cartilage organoid, whereas downregulated it in the 2D culture (Fig. 5D–G). Thus, the regulatory role of primary cilia in ECM deposition differed between the condylar cartilage organoid and 2D culture chondrocytes.

Primary cilia are known to regulate ECM deposition through their associated ion channels and HH signaling [22,24–27]. According to the heatmap, *TRPV4* and most HH signaling pathway-related genes were upregulated in the condylar cartilage organoid compared with the 2D culture system (Fig. 4C and D). The protein–protein interaction network also unveiled the link between *IFT88* and HH signaling pathway-related genes (Fig. 4E). As evidenced in western blotting, the protein levels of TRPV4 and HH signaling molecules (Patched 1 [PTCH1] and Indian hedgehog [Ihh]) increased in the condylar cartilage organoid compared with the 2D culture system (Fig. 6A and B). Moreover, the distribution of COL-X-, TRPV4-, and Ihh-positive areas in the condylar cartilage organoid and the natural condylar cartilage was similar (Fig. 6C). According to the quantification analysis of immunohistochemistry, COL-X, TRPV4, and Ihh protein levels in the superficial, proliferative, and hypertrophic zones of the condylar cartilage organoid and natural condylar cartilage were almost equivalent (Fig. 6D). To investigate the effects of *IFT88* knockdown on the protein levels of TRPV4 and HH signaling molecules in the condylar cartilage organoid, condylar chondrocytes were transiently transfected with *IFT88* siRNA. Western blotting demonstrated that *IFT88* knockdown upregulated the protein levels of TRPV4 and HH signaling molecules in the condylar cartilage organoid, whereas downregulated them in the 2D culture system (Fig. 6E–L). These results thus indicated that the regulatory role played by primary cilia in TRPV4 and HH singling pathways was different between the condylar cartilage organoid and 2D culture chondrocytes.

5. Primary cilia play different roles in ECM deposition in each zone of the condylar cartilage organoid

Considering that the average primary cilia length differed in each zone of the condylar cartilage organoid, we determined whether the regulatory role of primary cilia in ECM deposition also differed in each zone. Therefore, we constructed the si *IFT88* condylar cartilage organoid, which comprised chondrocytes with *IFT88* knockdown. Primary cilia length was compared between the condylar cartilage organoid and si *IFT88* condylar cartilage organoid through confocal microscopy. On average, primary cilia were shorter in the constructed si *IFT88* organoid than in the condylar cartilage organoid (Fig. 7A–C). The average primary cilia lengths in the proliferative and hypertrophic zones of the si *IFT88* condylar cartilage organoid significantly decreased compared with that in the control condylar cartilage organoid (Fig. 7A–C). Moreover, the average primary cilia length in the three zones of the si *IFT88* condylar cartilage organoid was similar (Fig. 7 A, B, C).

HE staining revealed that the thickness of the superficial zone increased, while the thickness of the proliferative and hypertrophic zones decreased in the si *IFT88* condylar cartilage organoid (Fig. 7D). Meanwhile, chondrocytes in the superficial zone were

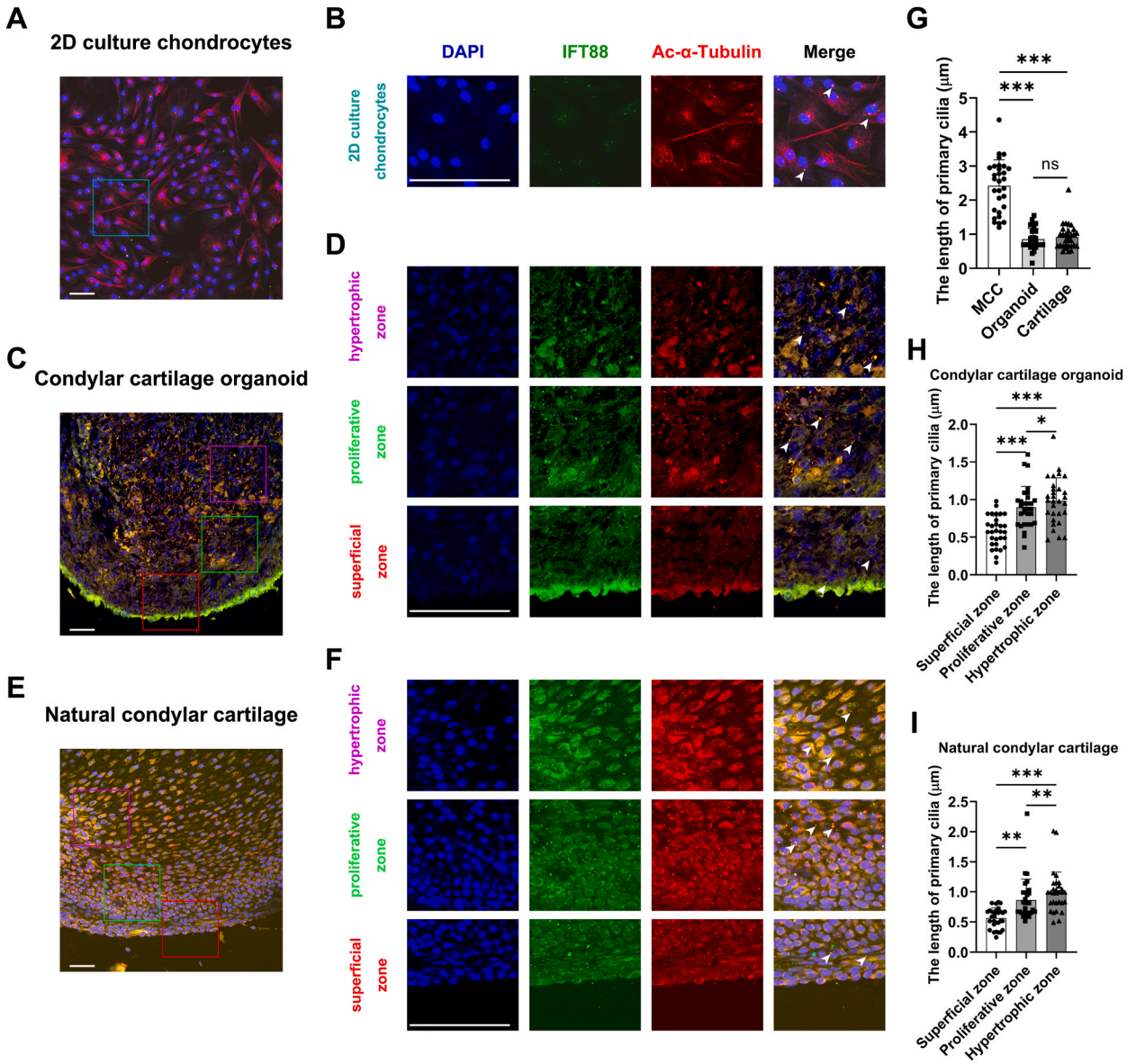

Fig. 2. The characteristics of primary cilia in condylar cartilage organoid and 2D culture chondrocytes.
(A and B) Immunofluorescence of IFT88 (green) and Ac-α-Tubulin (red) in 2D chondrocyte culture. (C) Immunofluorescence of IFT88 (green) and Ac-α-Tubulin (red) in condylar cartilage organoid. (D) Immunofluorescence of IFT88 (green) and Ac-α-Tubulin (red) in the superficial zone, proliferative zone, and hypertrophic zone of condylar cartilage organoid. (E) Immunofluorescence of IFT88 (green) and Ac-α-Tubulin (red) in rat condylar cartilage. (F) Immunofluorescence of IFT88 (green) and Ac-α-Tubulin (red) in the superficial zone, proliferative zone, and hypertrophic zone of natural condylar cartilage. (G) The length of primary cilia is measured and compared among 2D culture chondrocytes, condylar cartilage organoid, and natural condylar cartilage by ImageJ. (H and I) The length of primary cilia was measured and compared among the superficial zone, proliferative zone, and hypertrophic zone of condylar cartilage organoid and natural condylar cartilage. The length of cilia is measured from at least 3 different fluorescent micrographs from each independent experiment by using the ImageJ straight-line tool. Arrowheads: primary cilia. The data for quantification are sourced from 3 independent experiments. The data are presented as the mean ± SD (n = 3). *P < 0.05; **P < 0.01; ***P < 0.001, ns: not significant. MCC: 2D culture mandibular condylar chondrocytes. Scale bars = 100 μm.

hypertrophic in the constructed si *IFT88* condylar cartilage organoid compared with the condylar cartilage organoid (Fig. 7D). According to Safranin O staining, aggrecan distribution increased in the superficial zone of the constructed si *IFT88* condylar cartilage organoid compared with the condylar cartilage organoid (Fig. 7E). Immunohistochemical staining also unveiled that the COL-X protein level increased in the superficial zone of the si *IFT88* condylar cartilage organoid compared with the condylar cartilage organoid. However, the protein level of COL-X in the proliferative and hypertrophic zones of si *IFT88* condylar cartilage organoid were not significantly altered compared with the condylar cartilage organoid (Fig. 7F). These results indicated that the regulatory role of

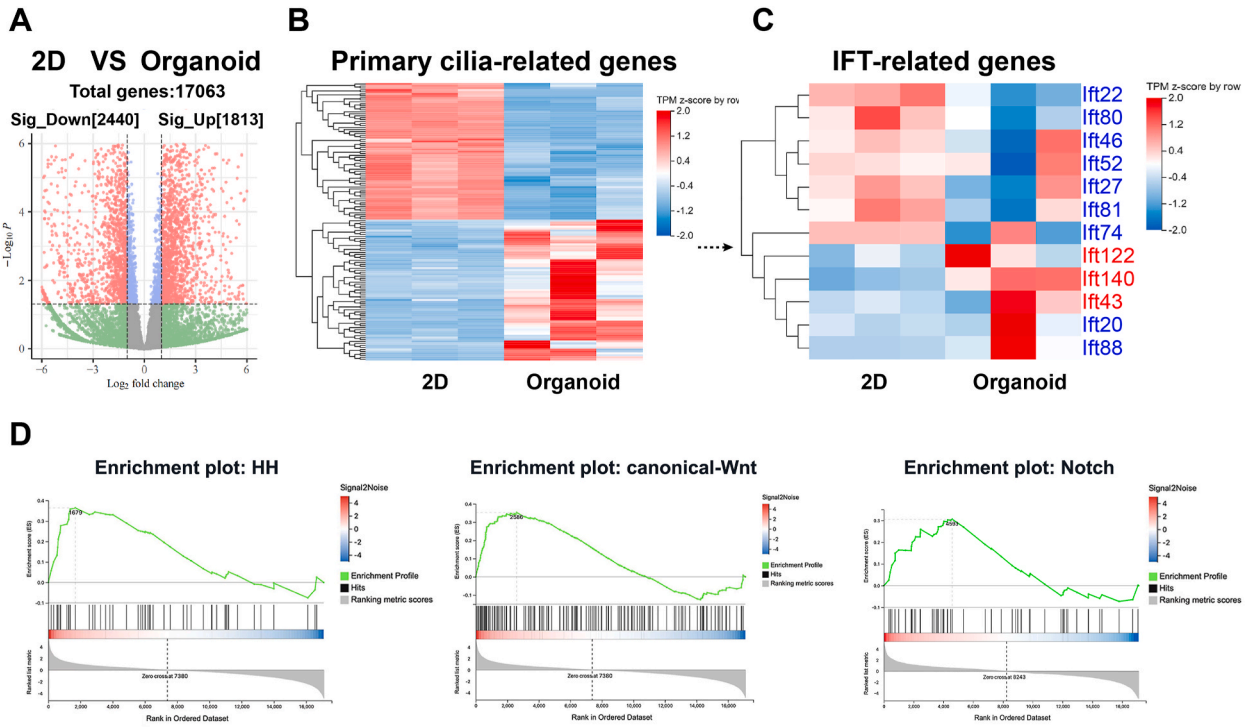

Fig. 3. RNA-seq analysis of cilia-related genes and signaling pathways in condylar cartilage organoid.
(A) Volcano plots of the differentially expressed genes in 2D culture chondrocytes versus condylar cartilage organoid (fold change >2, adjusted P < 0.05). (B) Heatmap displays the expression of primary cilia-related genes between 2D culture chondrocytes and condylar cartilage organoid. (C) Heatmap displays the expression of IFT-related genes between 2D culture chondrocytes and condylar cartilage organoid. The red indicates IFT-A complex genes; the blue indicates IFT-B complex genes. (D) GSEA reveals that the expression levels of primary cilia-related signaling pathways such as the HH, canonical-Wnt, and Notch are upregulated in condylar cartilage organoid when compared to that in 2D culture chondrocytes.

primary cilia in ECM deposition differed in each zone of the condylar cartilage organoid.

Considering that primary cilia-mediated regulation of ECM deposition was associated with ion channels and HH signaling, we determined whether the effects of *IFT88* knockdown on the protein levels of TRPV4 and HH signaling molecules (PTCH1, Ihh) also differed in each zone of the condylar cartilage organoid. According to the immunohistochemical staining, the levels of the aforementioned protein and signaling molecules increased in the superficial zone of si *IFT88* condylar cartilage organoid compared with the condylar cartilage organoid (Fig. 7G; Figs. S1A and B). Moreover, the protein levels of TRPV4 and HH signaling molecules in the proliferative and hypertrophic zones of si *IFT88* condylar cartilage organoid were not significantly different from those in the proliferative and hypertrophic zones of the condylar cartilage organoid (Fig. 7G; Figs. S1A and B). When the immunohistochemical results were quantitatively analyzed, we noted that COL-X, Ihh, PTCH1, and TRPV4 protein levels increased in the si *IFT88* condylar cartilage organoid compared with the control organoid (Fig. 7H and I; Figs. S1C and D). These results indicated that the regulatory role of primary cilia in TRPV4 and HH singling pathways also differed in each zone of the condylar cartilage organoid.

3. Discussion

We here constructed a novel condylar cartilage organoid consisting of superficial, proliferative, and hypertrophic zones. This organoid was similar to the natural condylar cartilage. Moreover, in the condylar cartilage organoid, chondrocytes were encapsulated in the ECM comprising aggrecan, type II collagen, and COL-X. Therefore, the condylar cartilage organoid better recapitulated the natural environment of the chondrocytes than the 2D culture chondrocytes. Thus, it served as a suitable model for investigating the biological functions of chondrocytes.

The reason for the difference in the regulatory role of primary cilia between the organoid and 2D culture remains unclear. This discrepancy may be attributable to differences in cell types and cellular density. First, diverse cell types within organoids (superficial, proliferative, and hypertrophic chondrocytes) distinctly separate them from 2D cultures. This cellular diversity causes variations in primary cilia length, the expression of cilia-related genes, and the interaction of cilia-related signaling pathways in the organoid compared with the 2D culture. Second, cellular density within organoids is notably higher than that of the density of chondrocytes in 2D cultures. Cellular density also varies across different zones within the organoid. Thus, changes in cellular density may play a crucial role in shaping gene expression patterns. Both cellular varieties and density play critical roles in modulating gene expression and signaling transduction. However, which factor is more crucial is difficult to determine. In the future, comprehensive analyses will be

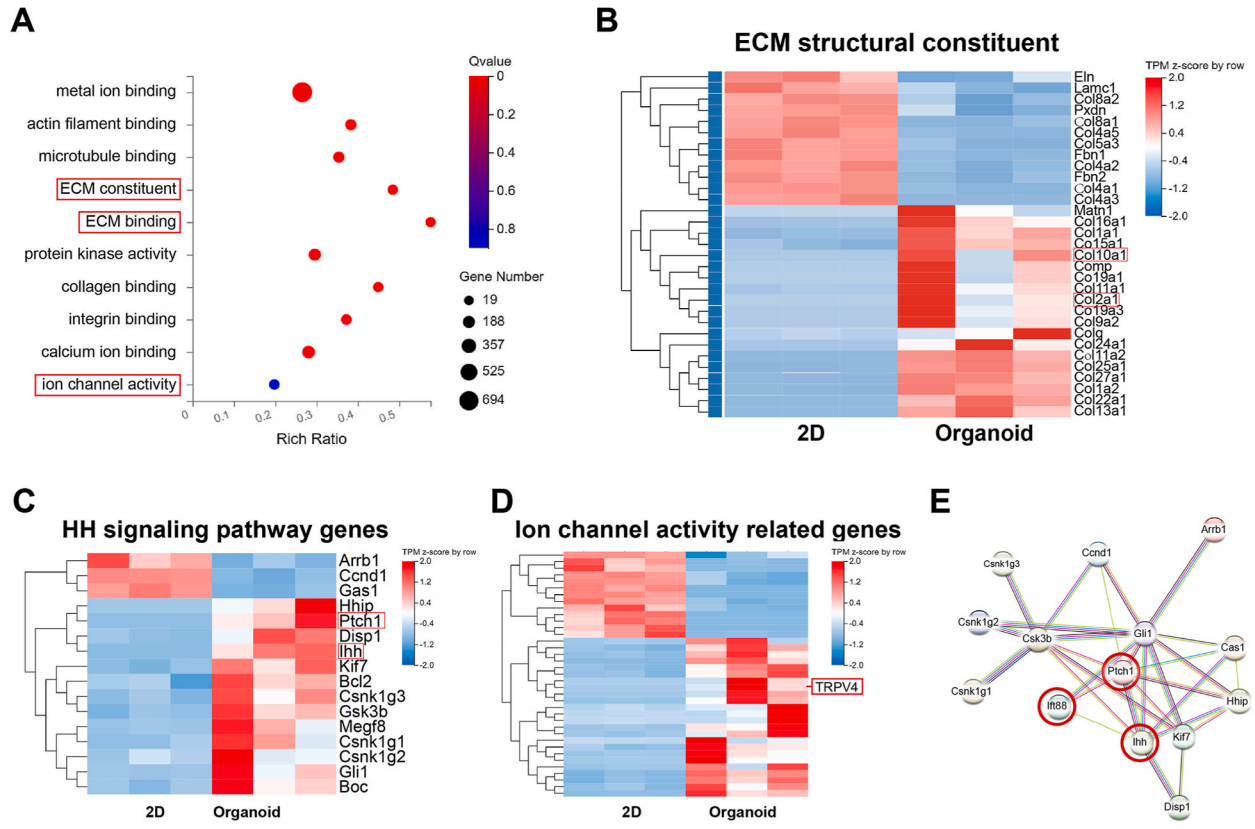

Fig. 4. RNA-seq analysis of ECM-related genes and cilia-related ion channels and HH signaling genes in condylar cartilage organoid.
(A) Gene ontology analysis in 2D culture chondrocytes and condylar cartilage organoid. (B) Heatmap displays the expression of ECM constituent related genes between 2D culture chondrocytes and condylar cartilage organoid. (C) Heatmap displays the expression of HH signaling pathway genes between 2D culture chondrocytes and condylar cartilage organoid. (D) Heatmap displays the expression of ion channel activity related genes between 2D culture chondrocytes and condylar cartilage organoid. (E) Protein-protein interaction network demonstrates the interaction between IFT88 and HH signaling pathway related genes.

conducted to discern the relative contributions of cellular varieties and density to these gene expression patterns.

Studies have constructed knee cartilage organoids using bovine or porcine chondrocytes [12,28,29]. However, these organoids had some disadvantages. First, obtaining bovine or porcine chondrocytes is difficult and expensive. Second, experimental results cannot be easily reproduced *in vivo* based on bovine- or porcine-derived organoid cartilage because feasible laboratory outposts for such large animals are lacking. Third, related bovine- or porcine tissue-targeting antibodies for subsequent experiments are lacking. The condylar cartilage organoid constructed in the present study offers unique advantages compared with the other cartilage models. First, our organoid was constructed using condylar chondrocytes from SD rats, which are cheaper and more convenient to obtain. Second, experimental results obtained using the condylar cartilage organoid can be easily reproduced *in vivo*.

In the condylar cartilage organoid, primary cilia were shortened, but the protein levels of the cilia-related HH signaling molecules (PTCH1 and Ihh) increased. These results are contradictory to those of a previous study. In that study, primary cilia shortening decreased the protein levels of the aforementioned signaling molecules in 2D culture chondrocytes [2]. Considering that the *in vivo* and *in vitro* primary cilia-related results are always contradictory, the impact of IFT88 knockdown on HH signaling molecules was compared between the constructed organoid and 2D culture systems. IFT88 knockdown increased the PTCH1 and Ihh protein levels in the condylar cartilage organoid, whereas downregulated them in the 2D culture system. In some studies, many cartilage-specific *IFT88*-cKO mice were created to investigate the regulatory role of primary cilia in cartilage. The expression of COL-X and HH signaling molecules (such as PTCH1) increased in Col2aCre; *IFT88* $^{fl/fl}$ mice compared to wild-type mice, similar to the results obtained for our si *IFT88* condylar cartilage organoid [30]. Additionally, in the aggrecanCreERT2; *IFT88* $^{fl/fl}$ mice, the expression of HH signaling molecules also increased [31]. Therefore, we consider that the condylar cartilage organoid is a more appropriate model for exploring primary cilia.

Notably, *IFT88* knockdown inhibited ECM deposition in the hypertrophic and proliferative zones of condylar cartilage organoid, whereas it promoted ECM deposition in its superficial zone. Additionally, primary cilia were longer in the hypertrophic and proliferative zones than in the superficial zones within the condylar cartilage organoid. Accordingly, we speculate that changes in primary cilia length may be a crucial reason for the different regulatory roles of primary cilia in ECM deposition. However, this hypothesis requires further research.

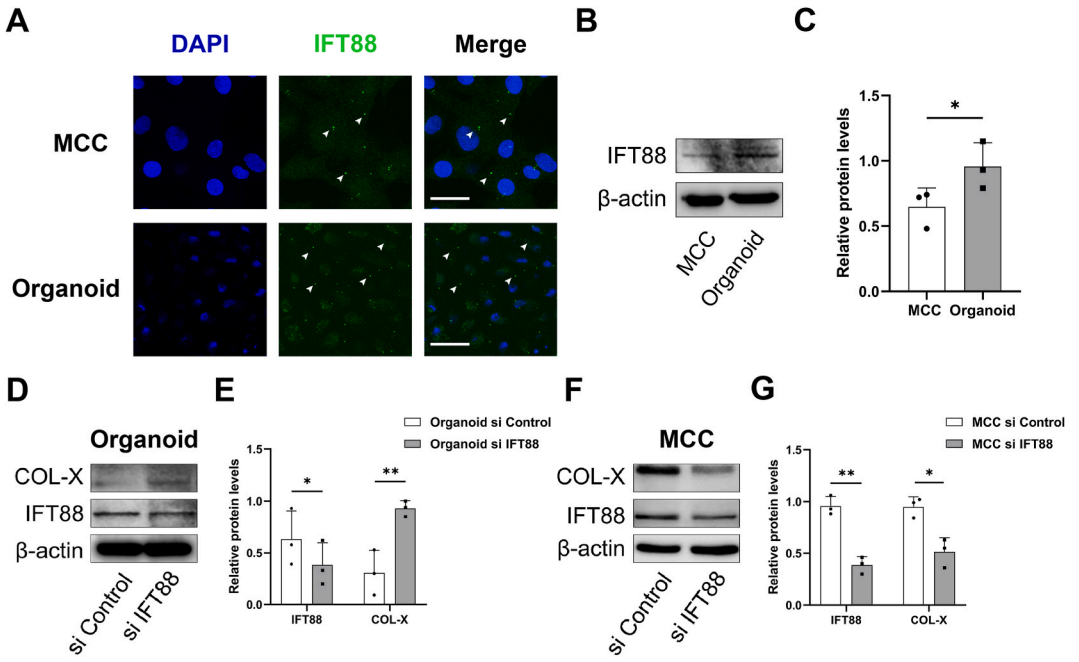

Fig. 5. Primary cilia show the opposite impact on ECM deposition between condylar cartilage organoid and 2D culture chondrocytes.
(A) The immunofluorescence of IFT88 in condylar cartilage organoid and 2D culture chondrocytes. Arrowheads: IFT88. (B) Western blotting of IFT88 in condylar cartilage organoid and 2D culture chondrocytes. (C) The relative protein expression levels of IFT88 are compared between condylar cartilage organoid and 2D culture chondrocytes by ImageJ. (D) Western blotting of IFT88 and COL-X in *IFT88* siRNA-treated and controlled condylar cartilage organoid. (E) The relative protein expressions are compared between *IFT88* siRNA-treated and control condylar cartilage organoid by ImageJ. (F) Western blotting of IFT88 and COL-X in *IFT88* siRNA-treated and control 2D culture chondrocytes. (G) The relative protein expressions are compared between *IFT88* siRNA-treated and control 2D culture chondrocytes by ImageJ. The data for quantification are sourced from 3 independent experiments. The data are presented as the mean ± SD (n = 3). *P < 0.05; **P < 0.01. MCC: 2D culture mandibular condylar chondrocytes. Scale bars = 50 μm.

Our study has several limitations. The condylar cartilage organoid could not mimic the condylar cartilage development process. This is because many types of cells such as osteocytes and synoviocytes regulate the growth, ossification, and regeneration of the condylar cartilage [32–34]. The condylar cartilage organoid could not be used to investigate the interaction among chondrocytes, osteoblasts, and synoviocytes. Therefore, future studies will focus on establishing an organoid co-culture model of the temporomandibular joint consisting of chondrocytes, osteoblasts, and synoviocytes. This may remarkably facilitate the study of temporomandibular joint development and diseases.

Collectively, we constructed a novel condylar cartilage organoid, which authentically recapitulates the structure of the natural condylar cartilage. The regulatory role of primary cilia in the condylar cartilage organoid is more similar to that in the natural condylar cartilage. This indicated that the condylar cartilage organoid is suitable for exploring primary cilia functions in the condylar cartilage.

Funding statement

This study was supported by the "National Key Research and Development Program of China [grant No. 2022YFC2405404]" to Xuewen Yang and "Knowledge Innovation Program of Wuhan -Basi Research, Shugung Project [grant No. 2022020801020504]" to Guoliang Sa.

Declaration of interest's statement

There are no competing financial or non-financial interests in relation to the work described.

Ethics approval and consent to participate

The animal protocol used in this study was approved by the Medical Ethics Committee of the Hospital of Stomatology, Wuhan University (No. S07922040B). All animal procedures were performed in accordance with the guidelines of the ARRIVE 2.0 checklist.

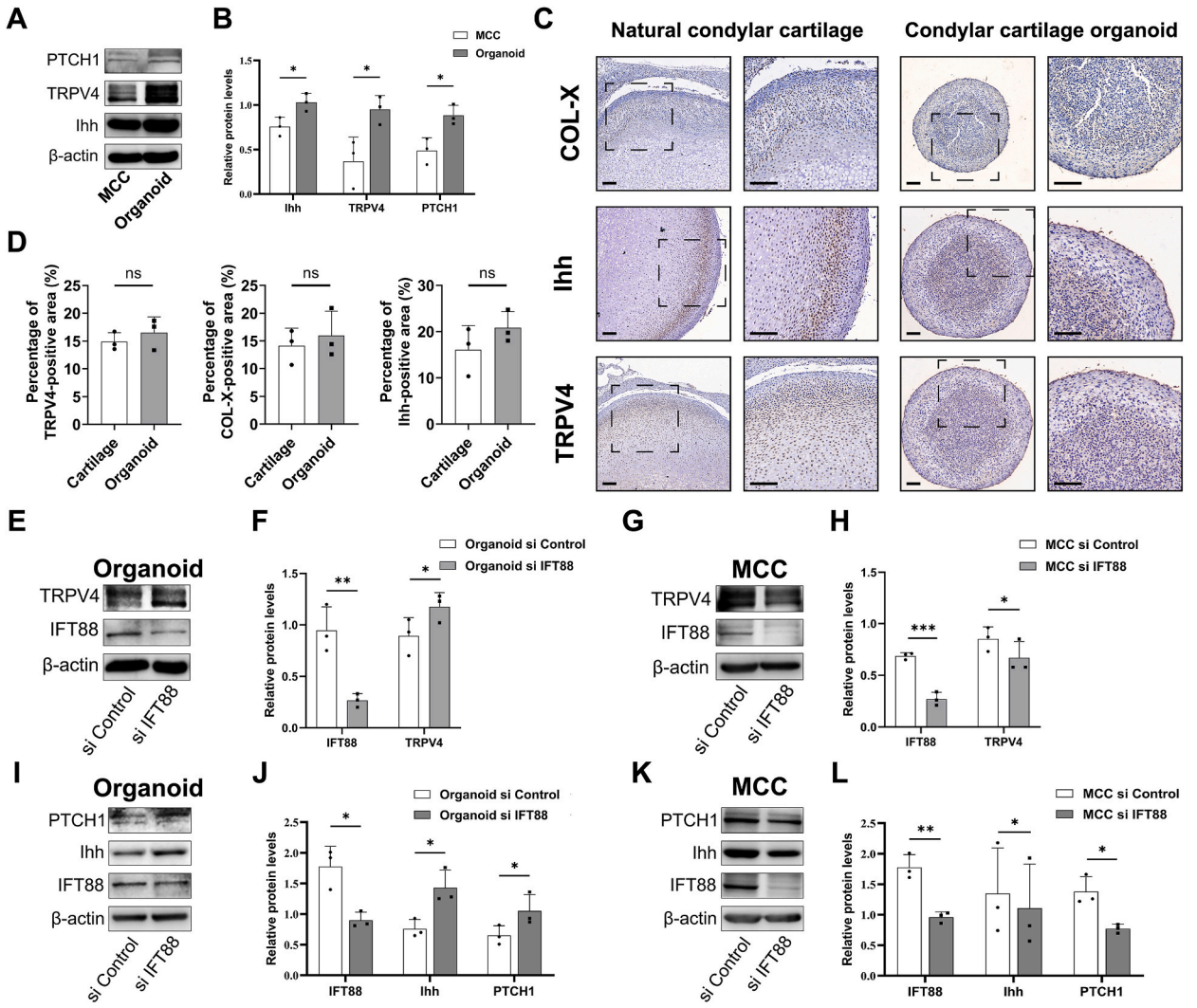

Fig. 6. The effects of primary cilia on TRPV4 and HH singling pathways between condylar cartilage organoids and 2D culture chondrocytes. (A, B) Western blotting of TRPV4, PTCH1, and Ihh in condylar cartilage organoid and 2D culture chondrocytes, and their statistical analyses. (C) Immunohistochemical staining results show COL-X, Ihh, and TRPV4 positive staining concentrates in the proliferative zone of natural condylar cartilage and IFT88 condylar cartilage organoid. (D) Quantitative data of the immunohistochemical signals of COL-X, Ihh, and TRPV4. (E, F) Western blotting of IFT88 and TRPV4 in *IFT88* siRNA-treated and control condylar cartilage organoid, and their statistical analyses. (G, H) Western blotting of IFT88 and TRPV4 in *IFT88* siRNA-treated and control 2D culture chondrocytes, and their statistical analyses. (I-J) Western blotting of IFT88, PTCH1, and Ihh in *IFT88* siRNA-treated and control condylar cartilage organoid, and their statistical analysis. (K, L) Western blotting of IFT88, PTCH1, and Ihh in *IFT88* siRNA-treated and control 2D culture chondrocytes, and their statistical analysis. The data for quantification are sourced from 3 independent experiments. Arrowheads: IFT88. The data are presented as the mean ± SD (n = 3). *P < 0.05; **P < 0.01; ***P < 0.001. MCC: 2D culture mandibular condylar chondrocytes. Scale bars = 100 μm.

Data availability

The RNA sequencing data are uploaded to GEO (GSE230630).

All data needed to evaluate the conclusions in the paper are present in the paper and/or the Supplementary Materials. Any additional information required to reanalyze the data reported in this paper is available from the lead contact upon reasonable request.

Methods

Animals

A total of 24 neonatal SD rats were purchased from Hubei Experimental Animal Research Center (Wuhan, China) [License No. SCXK

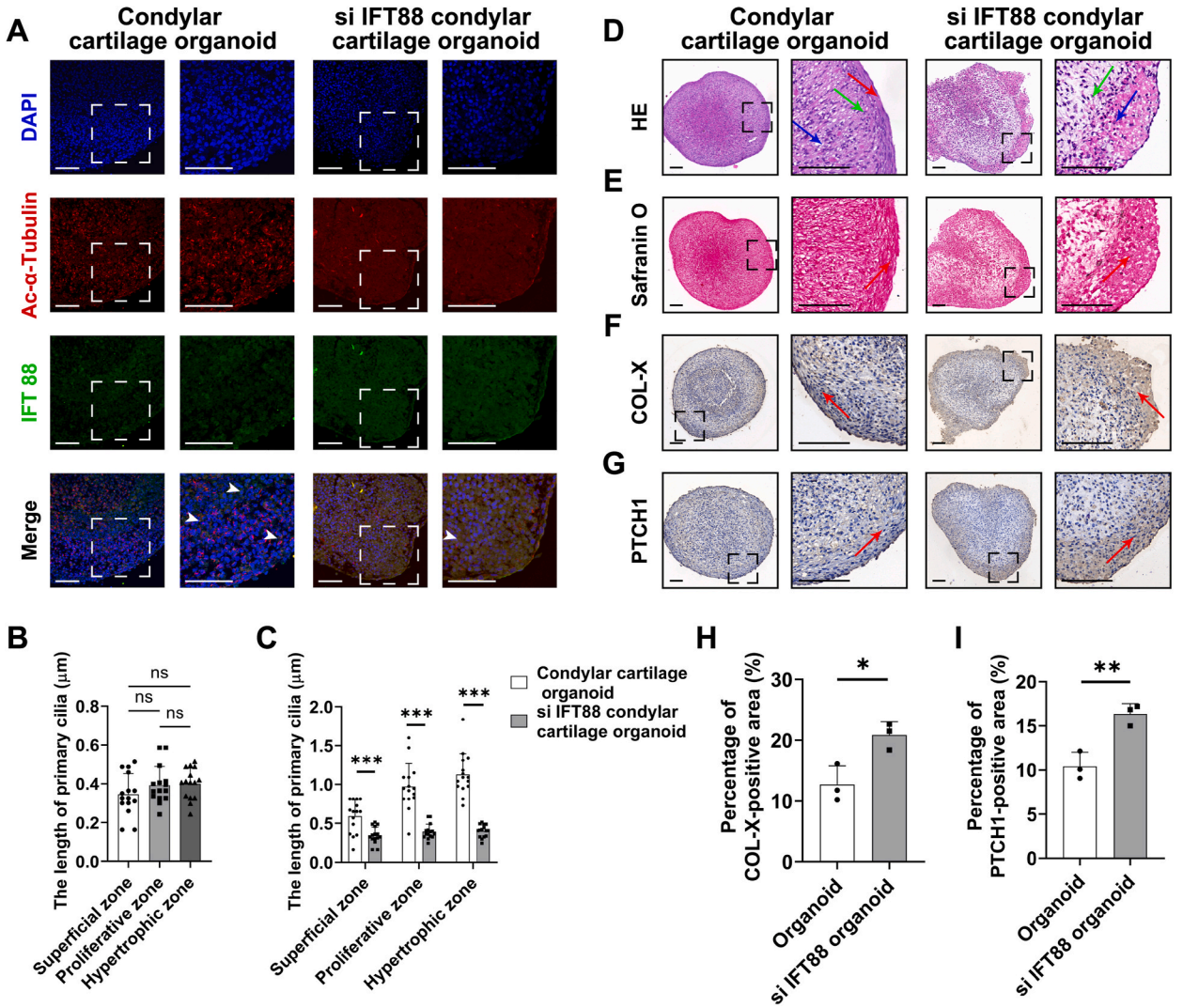

Fig. 7. The effects of primary cilia on COL-X, TRPV4 and HH singling molecules in each zone of condylar cartilage organoid.
(A) The immunofluorescence of IFT88 (green) and Ac-α-Tubulin (red) in condylar cartilage organoid and si *IFT88* condylar cartilage organoid. (B) The length of primary cilia was measured and compared among the superficial zone, proliferative zone, and hypertrophic zone of si *IFT88* condylar cartilage organoid. (C) The length of primary cilia was compared among the superficial zone, proliferative zone, and hypertrophic zone of condylar cartilage organoid and si *IFT88* condylar cartilage organoid. (D) HE staining of condylar cartilage organoid and si *IFT88* condylar cartilage organoid. (E) Safranin O staining indicates that aggrecan in the superficial zone of si *IFT88* condylar cartilage organoid is increased compared to condylar cartilage organoid. (F) Immunohistochemical staining results show COL-X positive staining concentrates in the superficial zone of si *IFT88* condylar cartilage organoid. (G) Immunohistochemical staining results show PTCH1 positive staining concentrates in the superficial zone of si *IFT88* condylar cartilage organoid. (H–I) Quantitative data of the immunohistochemical signals of COL-X, PTCH1, Ihh, and TRPV4. Red, green, and blue arrows indicate the superficial zone, proliferative zone, and hypertrophic zone, respectively. Arrowheads: primary cilia. The length of cilia is measured from at least 3 different fluorescent micrographs from each independent experiment by using the ImageJ straight-line tool. Scale bars = 100 μm.

(E) 2010–0009]. The rat mandibular condylar cartilage tissue from 24 SD rats were divided randomly into 3 groups: natural condylar cartilage, condylar cartilage organoid, and 2D culture chondrocytes. No significant difference was detected between males and females. Neonatal SD rats were euthanized by CO_2 asphyxiation. The animal protocol used in this study was approved by the Medical Ethics Committee of the Hospital of Stomatology, Wuhan University (No. S07922040B). All animal procedures were performed in accordance with the guidelines of the ARRIVE 2.0 checklist.

Isolation and culture of mandibular condylar chondrocytes of SD rats

Condylar chondrocytes were isolated as previously described [35] from neonatal SD rats (the first day after birth). The rat mandibular condylar cartilage tissue was isolated from the condylar bone-cartilage junction in neonatal SD rats under a

stereomicroscope. Isolated condylar chondrocytes were identified through morphological evaluation and type II collagen immunocytochemical staining, as described previously [36]. The dissected cartilage tissue was digested using 0.2 % type II collagenase (Gibco) for 3–4 h at 37 °C. After passing the solution through a 70-μm cell strainer (Falcon, Corning), the solution was centrifuged at 1000 rpm for 5 min to terminate digestion. The precipitate was resuspended in T25 plastic flasks (NEST, Beijing, China) containing Dulbecco's Modified Eagle's Medium (DMEM, Hyclone, Logan, UT, USA) supplemented with 20 % fetal bovine serum (Vivacell, Shanghai, China). The primary cells at passage 0 were cultured at 37 °C in an incubator under 5 % CO_2. When the confluence rate reached 80 %, the cells at passage 0 were averagely seeded onto two T25 plastic flasks, which were termed passage 1. Similarly, the cells at passage 1 were averagely seeded onto two new T25 plastic flasks, which were termed as passage 2 and were used for subsequent experiments.

Construction of condylar cartilage organoid

Each well of a 96-well plate was cleaned three times with phosphate-buffered saline (PBS). Then, molecular biology-grade agarose (2 % weight/volume PBS) was boiled, and 100 μL of the agarose was added to the wells before it was solidified. Moreover, the plates were tilted to spread the agarose along the walls and then inverted to remove the excess agarose. Chondrocyte culture media were presaturated with chondrogenic medium (20 % fetal bovine serum (Vivacell); DMEM with GlutaMAX (Gibco); 1 % nonessential amino acids (0.1 mM) (Gibco); 1 % insulin, human transferrin, and selenous acid (ITS+; BD Biosciences); dexamethasone (100 nM) (Sigma-Aldrich); ascorbate-2-phosphate (50 μg/mL) (Sigma-Aldrich); and sodium pyruvate (100 μg/mL) (Sigma-Aldrich) and L-proline (40 μg/mL) (Sigma-Aldrich) [12,28]. In the non-adherent agarose wells, 2.5 million cells were mixed with 200 μL of culture media. At the bottom of each well, condylar chondrocytes gradually formed self-assembled, scaffold-free, condylar cartilage organoid constructs in 7–10 days. Each day, 400 μL of media was changed (200 μL twice daily).

Histological analysis

The condylar cartilage organoid and natural condylar cartilage were fixed in 4 % paraformaldehyde (PFA) solution at 4 °C for 24 h. After being embedded in paraffin, 4-μm sagittal sections were made (Leica RM2245. Wetzlar, Germany). Tissue sections were deparaffinated using xylene and rehydrated with hydrous ethanol series. The sections were then stained using hematoxylin and eosin (HE), Safranin O and Sirius Red.

Immunohistochemistry

Tissue sections were deparaffinated using xylene and rehydrated with hydrous ethanol series, followed by antigen retrieval solution (C1034, Solarbio, China) incubation for 15 min at 95 °C. Then, to block the endogenous peroxidase activity, sections were incubated with 3 % hydrogen peroxide for 10 min at room temperature. Tissue sections were blocked with 3 % bovine serum albumin for 1 h at 37 °C and then incubated with the primary antibody targeting COL2A1 (ab34712, Abcam, China) overnight at 4 °C. Then appropriate secondary antibodies (Beyotime, Shanghai, China) were applied subsequently. Finally, the sections were stained with 3,3′-diaminobenzidine (DAB; Sigma) and covered. Negative controls were obtained by omitting the primary antibodies.

The images obtained from COL-X, PTCH1, Ihh, and TRPV4 immunohistochemistry were analyzed using ImageJ; thresholds of 0 and 160 were used to quantify the COL-X-, PTCH1-, Ihh-, and TRPV4-positive area. We calculated the percentage of the condylar cartilage organoid, si *IFT88* condylar cartilage organoid, and natural condylar cartilage area which was COL-X-, PTCH1-, Ihh-, and TRPV4–positive.

Total RNA extraction and sequencing

To explore the characteristics of transcriptomics of 2D culture chondrocytes and condylar cartilage organoid, total RNA was extracted from the cells and tissues respectively using Trizol reagent (Life technologies, New York, USA) according to manual instruction. Six samples (three samples of 2D culture condylar chondrocytes and three condylar cartilage organoid) were sequenced at BGI (Wuhan, China) using transcriptome sequencing technology.

Pathway and Functional enrichment analyses

The sequencing data was filtered with SOAPnuke (v1.5.2) by Removing reads containing sequencing adapter; (2) Removing reads whose low-quality base ratio (base quality less than or equal to 5) is more than 20 %; (3) Removing reads whose unknown base ('N' base) ratio is more than 5 %, afterwards clean reads were obtained and stored in FASTQ format. The clean reads were mapped to the reference genome using HISAT2 (v2.0.4) [37]. After that, Ericscript (v0.5.5) [38] and rMATS (V3.2.5) [39] were used to fusion genes and differential splicing genes (DSGs), respectively. Bowtie2 (v2.2.5) [40] was applied to align the clean reads to the gene set, a database for this organism built by BGI (Beijing Genomic Institute in ShenZhen), which known and novel, coding transcripts were included, then expression level of gene was calculated by RSEM (v1.2.12). The heatmap was drawn by pheatmap (v1.0.8) [41] according to the gene expression in different samples. Essentially, differential expression analysis was performed using the DESeq2 (v1.4.5) with Q value $\leq$ 0.05. To take insight to the change of phenotype, GO (http://www.geneontology.org/) enrichment analysis of annotated different expression gene was performed by Phyper (https://en.wikipedia.org/wiki/Hypergeometric_distribution) based on Hypergeometric test. The significant levels of terms and pathways were corrected by Q value with a rigorous threshold (Q value $\leq$

0.05) by Bonferroni. Gene set enrichment analysis (GSEA) was performed using GSEA software (version 4.3.2). The significant levels of terms and pathways were corrected by Q value with a rigorous threshold (Q value $\leq$ 0.05) by Bonferroni.

SiRNA transfection

Using IFT88 siRNA (CCAACGACCUGGAGAUUAATT) purchased from GenePharma (Suzhou, China), transfection was performed when the cell density achieved 70 % confluency. The cells were transfected using the Lipofectamine 3000 system (Invitrogen, Thermo Fisher Scientific, USA) with siRNAs or control siRNAs. In the 2D culture system, after the chondrocytes were transfected for 72 h, the transfection efficacy was analyzed through western blotting. In organoid culture, after the chondrocytes were transfected for 24 h, these chondrocytes were seeded into agarose wells to construct si *IFT88* condylar cartilage organoid.

Western blotting analysis

The cells were lysed in RIPA buffer (Beyotime, Shanghai, China) with a protease inhibitor cocktail (Roche, Mannheim, Germany). The condylar cartilage organoids and si *IFT88* condylar cartilage organoids were harvested from agarose on the 7th day and then were ground into a paste before being lysed in RIPA buffer with a protease inhibitor cocktail. The quantification of proteins in collected lysates was conducted using a Bicinchoninic acid kit (Beyotime, Shanghai, China). The protein samples were subjected to 10 % sodium dodecyl sulfate-polyacrylamide gel (Bio-Rad) and then transferred to polyvinylidene difluoride membranes (Millipore, Billerica, MA, USA). After blocking with 5 % nonfat milk for 1 h, the membranes were first incubated with primary antibodies overnight at 4 °C and then incubated with appropriate secondary antibodies (1:10,000; ABclonal, Wuhan, China) for 1 h. The antibodies used are shown in Additional file 1. The immunoblots on the membrane were developed with an Enhanced Chemiluminescence kit (Advansta Inc., San Jose, CA, USA) and visualized using a chemiluminescence Odyssey Fc Imaging System (LI-COR Biosciences, Lincoln, NE, USA). A semiquantitative analysis of Western blots was carried out using Image J software as following: 1) The image was opened. 2) The image was converted into a grayscale picture. 3) The background was subtracted. 4) The integrated density was set. 5) Scales were set. 6) The image was inverted into a bright band. 7) The integrated gray values of the respective bands were acquired by freehand selection. The Western blot densities of indicated proteins were normalized with β-actin. Then, the fold changes were determined by calculating the ratio of indicated proteins to those of 2D culture mandibular condylar chondrocytes (MCC), MCC Si Control, and condylar cartilage organoid Si Control (the protein levels of MCC, MCC Si Control, and condylar cartilage organoid Si Control were set at 1).

Immunofluorescence

Mandibular condylar chondrocytes were first fixed with 4 % paraformaldehyde for 15 min, and then they were permeabilized with 0.3 % Triton for 15 min. The condylar cartilage organoid and condylar cartilage were fixed in 4 % PFA solution at 4 °C for 24 h. After being embedded in paraffin, 4-μm sagittal sections were made (Leica RM2245. Wetzlar, Germany). Tissue sections were deparaffinated using xylene and rehydrated with hydrous ethanol. Tissue sections and chondrocytes samples were blocked with 3 % bovine serum albumin for 1 h and then incubated with the primary antibody targeting acetylated-α-tubulin (or IFT88 and TRPV4) overnight at 4 °C. The information of antibodies used for immunofluorescence is presented in Table S1. The samples were washed thrice with PBS, and goat anti-rabbit Alexa Fluor® 594 or 488-conjugated secondary antibody (1:200) was applied in a dark chamber for 1 h at 37 °C. Finally, these samples were stained with 1 μg/mL 4',6-diamidino-2-phenylindole (DAPI) for 5 min and photographed using a Leica SP8 confocal microscope (Leica Microsystems, Wetzlar, Germany; or OLYMPUS Corporation, Japan).

The measurement of primary cilia length

The co-staining of Ac-α-Tubulin and IFT88 was used to identify primary cilia. The length of primary cilia was measured from at least 5 different fluorescent micrographs from each independent experiment using the Image J straight-line tool. A straight line was determined at the top and base of the cilia and automatically calculated by the software in pixels. The pixel value was converted to length in micrometers according to actual scale. The cilia prevalence was calculated by dividing the number of cells that contain a primary cilium by the number of cells on each micrograph.

Statistical analysis

All data were analyzed using GraphPad Prism software 8.4.0 (GraphPad Software, Inc.) and presented as the arithmetic mean values ± standard deviation (SD). The statistical significance comparing the two groups was assessed using two-tailed, unpaired Student's t-tests. $P < 0.05$ was considered statistically significant.

CRediT authorship contribution statement

Zhan Liu: Writing – review & editing, Writing – original draft, Software, Resources, Project administration, Methodology, Investigation, Formal analysis, Data curation, Conceptualization. **Haoyu Zhou:** Writing – original draft, Software, Resources, Project administration, Methodology, Investigation, Formal analysis, Data curation. **Qingwei Wu:** Visualization, Resources, Methodology, Investigation, Data curation. **Tianhao Luo:** Investigation, Formal analysis, Data curation. **Hanlin Tu:** Software, Formal analysis, Data

curation. **Guoliang Sa:** Writing – review & editing, Writing – original draft, Supervision, Methodology, Investigation, Funding acquisition, Formal analysis, Data curation, Conceptualization. **Xuewen Yang:** Writing – review & editing, Writing – original draft, Supervision, Investigation, Funding acquisition, Formal analysis, Data curation, Conceptualization.

Declaration of competing interest

The authors declare that they have no known competing financial interests or personal relationships that could have appeared to influence the work reported in this paper.

Appendix B. Supplementary data

Supplementary data to this article can be found online at https://doi.org/10.1016/j.heliyon.2024.e35972.

References

[1] G. Rossi, A. Manfrin, M.P. Lutolf, Progress and potential in organoid research, Nat. Rev. Genet. 19 (2018) 671–687, https://doi.org/10.1038/s41576-018-0051-9.

[2] H. Wang, P.C. Brown, E.C.Y. Chow, et al., 3D cell culture models: drug pharmacokinetics, safety assessment, and regulatory consideration, Clin Transl Sci 14 (2021) 1659–1680, https://doi.org/10.1111/cts.13066.

[3] H. Kleinman, D. Philp, M. Hoffman, Role of the extracellular matrix in morphogenesis, Curr. Opin. Biotechnol. 14 (2003) 526–532, https://doi.org/10.1016/j.copbio.2003.08.002.

[4] C. Liu, Y. Liu, X. Xu, et al., Potential effect of matrix stiffness on the enrichment of tumor initiating cells under three-dimensional culture conditions, Exp. Cell Res. 330 (2015) 123–134, https://doi.org/10.1016/j.yexcr.2014.07.036.

[5] H.K. Vanyai, F. Prin, O. Guillermin, et al., Control of skeletal morphogenesis by the Hippo-YAP/TAZ pathway, Development 147 (2020), https://doi.org/10.1242/dev.187187.

[6] C. Moysidou, C. Barberio, R. Owens, Advances in engineering human tissue models, Front. Bioeng. Biotechnol. 8 (2020) 620962, https://doi.org/10.3389/fbioe.2020.620962.

[7] C. Corro, L. Novellasdemunt, V.S.W. Li, A brief history of organoids, Am J Physiol Cell Physiol 319 (2020) C151–C165, https://doi.org/10.1152/ajpcell.00120.2020.

[8] O. Chaudhuri, J. Cooper-White, P. Janmey, et al., Effects of extracellular matrix viscoelasticity on cellular behaviour, Nature 584 (2020) 535–546, https://doi.org/10.1038/s41586-020-2612-2.

[9] B. Ho, N. Pek, B. Soh, Disease modeling using 3D organoids derived from human induced pluripotent stem cells, Int. J. Mol. Sci. 19 (2018), https://doi.org/10.3390/ijms19040936.

[10] L. Broutier, A. Andersson-Rolf, C. Hindley, et al., Culture and establishment of self-renewing human and mouse adult liver and pancreas 3D organoids and their genetic manipulation, Nat. Protoc. 11 (2016) 1724–1743, https://doi.org/10.1038/nprot.2016.097.

[11] B. He, X. Yuan, A. Zhou, et al., Designer functionalised self-assembling peptide nanofibre scaffolds for cartilage tissue engineering, Expert Rev Mol Med 16 (2014) e12, https://doi.org/10.1017/erm.2014.13.

[12] J. Lee, L. Huwe, N. Paschos, et al., Tension stimulation drives tissue formation in scaffold-free systems, Nat. Mater. 16 (2017) 864–873, https://doi.org/10.1038/nmat4917.

[13] C. Gemmiti, R. Guldberg, Fluid flow increases type II collagen deposition and tensile mechanical properties in bioreactor-grown tissue-engineered cartilage, Tissue Eng. 12 (2006) 469–479, https://doi.org/10.1089/ten.2006.12.469.

[14] E.Y. Salinas, A. Aryaei, N. Paschos, et al., Shear stress induced by fluid flow produces improvements in tissue-engineered cartilage, Biofabrication 12 (2020) 045010, https://doi.org/10.1088/1758-5090/aba412.

[15] M. Chatterjee, P.M. Muljadi, N. Andarawis-Puri, The role of the tendon ECM in mechanotransduction: disruption and repair following overuse, Connect. Tissue Res. 63 (2022) 28–42, https://doi.org/10.1080/03008207.2021.1925663.

[16] I. Collins, A.K.T. Wann, Regulation of the extracellular matrix by ciliary machinery, Cells 9 (2020), https://doi.org/10.3390/cells9020278.

[17] A.C. Ernault, M. Kawasaki, B. Fabrizi, et al., Knockdown of Ift88 in fibroblasts causes extracellular matrix remodeling and decreases conduction velocity in cardiomyocyte monolayers, Front. Physiol. 13 (2022) 1057200, https://doi.org/10.3389/fphys.2022.1057200.

[18] N. Stevenson, The factory, the antenna and the scaffold: the three-way interplay between the Golgi, cilium and extracellular matrix underlying tissue function, Biol Open 12 (2023), https://doi.org/10.1242/bio.059719.

[19] C. Poole, C. Jensen, J. Snyder, et al., Confocal analysis of primary cilia structure and colocalization with the Golgi apparatus in chondrocytes and aortic smooth muscle cells, Cell Biol. Int. 21 (1997) 483–494, https://doi.org/10.1006/cbir.1997.0177.

[20] Z. Anvarian, K. Mykytyn, S. Mukhopadhyay, et al., Cellular signalling by primary cilia in development, organ function and disease, Nat. Rev. Nephrol. 15 (2019) 199–219, https://doi.org/10.1038/s41581-019-0116-9.

[21] N. Klena, G. Pigino, Structural biology of cilia and intraflagellar transport, Annu. Rev. Cell Dev. Biol. 38 (2022) 103–123, https://doi.org/10.1146/annurev-cellbio-120219-034238.

[22] F. Bangs, K. Anderson, Primary cilia and mammalian hedgehog signaling, Cold Spring Harb Perspect Biol 9 (2017), https://doi.org/10.1101/cshperspect.a028175.

[23] K. Kawata, K. Narita, A. Washio, et al., Odontoblast differentiation is regulated by an interplay between primary cilia and the canonical Wnt pathway, Bone 150 (2021) 116001, https://doi.org/10.1016/j.bone.2021.116001.

[24] Z. Chinipardaz, M. Liu, D.T. Graves, S. Yang, Role of primary cilia in bone and cartilage, J. Dent. Res. 101 (2022) 253–260, https://doi.org/10.1177/00220345211046606.

[25] M.A. Corrigan, G.P. Johnson, E. Stavenschi, et al., TRPV4-mediates oscillatory fluid shear mechanotransduction in mesenchymal stem cells in part via the primary cilium, Sci. Rep. 8 (2018) 3824, https://doi.org/10.1038/s41598-018-22174-3.

[26] T. Saigusa, Q. Yue, M.A. Bunni, et al., Loss of primary cilia increases polycystin-2 and TRPV4 and the appearance of a nonselective cation channel in the mouse cortical collecting duct, Am J Physiol Renal Physiol 317 (2019) F632–F637, https://doi.org/10.1152/ajprenal.00210.2019.

[27] C.L. Thompson, M. McFie, J.P. Chapple, et al., Polycystin-2 is required for chondrocyte mechanotransduction and traffics to the primary cilium in response to mechanical stimulation, Int. J. Mol. Sci. 22 (2021), https://doi.org/10.3390/ijms22094313.

[28] J. Crispim, K. Ito, De novo neo-hyaline-cartilage from bovine organoids in viscoelastic hydrogels, Acta Biomater. 128 (2021) 236–249, https://doi.org/10.1016/j.actbio.2021.04.008.

[29] G. Otarola, J. Hu, K. Athanasiou, Intracellular calcium and sodium modulation of self-assembled neocartilage using costal chondrocytes, Tissue Eng Part A 28 (2022) 595–605, https://doi.org/10.1089/ten.TEA.2021.0169.

[30] C.F. Chang, G. Ramaswamy, R. Serra, Depletion of primary cilia in articular chondrocytes results in reduced Gli3 repressor to activator ratio, increased Hedgehog signaling, and symptoms of early osteoarthritis, Osteoarthritis Cartilage 20 (2012) 152–161, https://doi.org/10.1016/j.joca.2011.11.009.
[31] C.R. Coveney, L. Zhu, J. Miotla-Zarebska, et al., Role of ciliary protein intraflagellar transport protein 88 in the regulation of cartilage thickness and osteoarthritis development in mice, Arthritis Rheumatol. 74 (2022) 49–59, https://doi.org/10.1002/art.41894.
[32] H. Guo, H. Li, Y. Feng, et al., Cross-talk between synovial fibroblasts and chondrocytes in condylar hyperplasia: an in vitro pilot study, Oral Surg Oral Med Oral Pathol Oral Radiol 131 (2021) 558–564, https://doi.org/10.1016/j.oooo.2020.08.020.
[33] R. Hinton, Y. Jing, J. Jing, J. Feng, Roles of chondrocytes in endochondral bone formation and fracture repair, J. Dent. Res. 96 (2017) 23–30, https://doi.org/10.1177/0022034516668321.
[34] L. Zhan, S. Guoliang, Z. Zhuoyu, et al., Regulatory role of primary cilia in oral and maxillofacial development and disease, Tissue Cell 88 (2024) 102389, https://doi.org/10.1016/j.tice.2024.102389.
[35] Q. Liu, Q. Wan, R. Yang, et al., Effects of intermittent versus continuous parathyroid hormone administration on condylar chondrocyte proliferation and differentiation, Biochem. Biophys. Res. Commun. 424 (2012) 182–188, https://doi.org/10.1016/j.bbrc.2012.06.106.
[36] Z. Wang, G. Sa, L. Zheng, et al., Intraflagellar transport protein 88 interacts with polycystin 2 to regulate mechanosensitive hedgehog signaling in mandibular condylar chondrocytes, Arch. Oral Biol. 143 (2022) 105548, https://doi.org/10.1016/j.archoralbio.2022.105548.
[37] D. Kim, B. Langmead, S. Salzberg, HISAT: a fast spliced aligner with low memory requirements, Nat. Methods 12 (2015) 357–360, https://doi.org/10.1038/nmeth.3317.
[38] S. Shen, J. Park, Z. Lu, et al., rMATS: robust and flexible detection of differential alternative splicing from replicate RNA-Seq data, Proc Natl Acad Sci U S A. 111 (2014) E5593–E5601, https://doi.org/10.1073/pnas.1419161111.
[39] B. Langmead, S. Salzberg, Fast gapped-read alignment with Bowtie 2, Nat. Methods 9 (2012) 357–359, https://doi.org/10.1038/nmeth.1923.
[40] B. Li, C. Dewey, RSEM: accurate transcript quantification from RNA-Seq data with or without a reference genome, BMC Bioinf. 12 (2011) 323, https://doi.org/10.1186/1471-2105-12-323.
[41] M. Love, W. Huber, S. Anders, Moderated estimation of fold change and dispersion for RNA-seq data with DESeq2, Genome Biol. 15 (2014) 550, https://doi.org/10.1186/s13059-014-0550-8.